J. Fluid Mech. (1976), *vol.* 74, *part* 2, *pp.* 251–267
Printed in Great Britain

Turbulence correlations in a compressible wake

By A. DEMETRIADES
Aeronutronic Ford Corporation, Newport Beach, California 92663

(Received 16 May 1975)

Space–time correlations have been measured in the turbulent supersonic wake behind a slender axisymmetric body. The data were obtained with two independently-positioned hot-wire anemometers, and interpreted with the aid of an extension of compressible anemometry theory. Comparison with earlier single-point Eulerian spectra showed a breakdown of Taylor's hypothesis near the wake edge, and thus also the expected differences in the scale lengths. The eddy convection speed appears equal to that of the mean flow, and the eddy shape is inclined to the wake axis, although it becomes nearly parallel to it at the wake edge. As a consequence, radial and longitudinal space correlation functions appear nearly equal. An upstream–downstream asymmetry was noted in the latter.

1. Introduction

The main impetus for the turbulence research in high-speed wakes that proliferated in the 1960s came from a need to learn something about the wake space–time correlation functions (Lane 1967). A substantial volume of work has indeed been reported, from which many of the outstanding features of such wakes can be now adequately described; ironically, however, there are still few, if any, data on the correlations themselves. Most previous correlation studies were limited, because experimental difficulties led to making major assumptions that are questionable. Two such assumptions are those of frozen turbulence and the direct space–time transformation, needed in order to obtain space correlations from Eulerian spectra. (For example, by invoking Taylor's hypothesis, the time auto-correlation function is often used to derive the space correlation function.) No regard was given to the correlations in the lateral direction, or concern expressed about the multi-modal nature of compressible turbulence. Of course, it is precisely questions such as these of turbulence decay, eddy velocity, isotropy and compressibility that need most attention, because they comprise most of the physics of the problem.

The two key experimental difficulties explain the dearth of data. Since space correlations can be obtained only by multi-point measurements, one must either perfect remote multi-point sensors (e.g. laser-Doppler velocimeters) or eliminate mutual aerodynamic interference in flow-immersible sensor arrays; neither of these two goals has been amply achieved. In a compressible wake, too, one must not only distinguish among correlations of the different modes, but must also demonstrate that any single mode can be measured independently of the other.

Symbol	Definition	Measured dependence on $\bar{x}$	Magnitude at $\bar{x} = 91$
L	Transverse scale	$\sim \bar{x}^{\frac{1}{2}}$	0·107 in. = 0·272 cm
$U(0)$	Axis velocity	$\sim (1-w)$	586 m s^{-1}
U_∞	External velocity	Constant	617 m s^{-1}
$\frac{U_\infty - u(0)}{U_\infty} = w$	Velocity defect	$\sim \bar{x}^{-\frac{2}{3}}$	0·05
$T(0)$	Axis temperature	$\sim (1-\theta)$	119 °K
$\frac{T(0) - T_\infty}{T_\infty} = \theta$	Temperature defect	$\sim \bar{x}^{-\frac{2}{3}}$	0·149
$\bar{y}$	R.M.S. wake radius	$\sim \bar{x}^{\frac{1}{2}}$	0·225 in. = 0·57 cm
$(C_D A)^{\frac{1}{2}}$	Wake drag diameter	Constant	0·085 in. = 0·216 cm

TABLE 1. Measured wake flow properties at station where correlations were observed ($\bar{x} = 91$). Data from Demetriades (1968*a*, *c*).

Point number	y (cm)	$\eta = \tilde{y}/L$	$\tilde{U}$	u'	T'
A	0 (axis)	0	1	0·019	0·059
B	0·152	0·822	0·763	0·023	0·071
C	0·305	1·56	0·409	0·019	0·072
D	0·457	2·32	0·135	0·012	0·061
E	0·61	3·09	0·006	~0	0·039
F	0·762	3·86	0	~0	0·012

TABLE 2. Location and properties of points along radius where correlations were measured. Data from Demetriades (1968*b*). Letters identify points on figure 1.

For example, when hot-wire anemometers are used, it is sometimes claimed that the velocity correlation alone can be measured if the wire overheat is kept 'high' (Fox 1968). It can, in fact, be shown from the simple algebra of hot-wire response (Morkovin 1956) that this condition is unattainable in a medium of fluctuating density.

2. Experiment design

The purpose of this experiment was to measure the space–time correlations of velocity and temperature fluctuations in an axisymmetric, dynamically equilibrated wake flow, without external gradients or heat transfer, but with a discernible compressibility effect. Such a wake flow has been generated in the supersonic wind tunnel at this laboratory, at Mach 3·0 and wake Reynolds number 1500–500, behind a long circular rod aligned with the flow. This wake has been studied since 1966, and its mean, intermittent and turbulence characteristics have been reported in the literature (Demetriades 1968*a–c*). To ensure a certain turbulence equilibration, the measurements reported here were made at the farthest downstream 'station', lying a distance $x = 9{\cdot}15$ in. (23·3 cm) behind the model base; in terms of the non-dimensional axial co-ordinate $\bar{x}$ (distance from

turbulence origin divided by wake drag diameter) this corresponds to $\bar{x} = 91$. The wake Reynolds number Re_w at that point is 500.

The measurements were limited to longitudinal and radial space–time correlations at that axial position. No angular correlations were studied during this series, and the radial stations of measurement were restricted to six. The breadth of the work was therefore considerably reduced, mainly because the experimental method is so laborious, as will be shown below. For example, a total of 180 different correlation traverses were needed to deduce the longitudinal and radial correlations of velocity and temperature at these six radial points.

Table 1 gives the flow characteristics at $\bar{x} = 91$, and table 2 the location of the six points along the radius both in dimensional (y in cm) and in non-dimensional terms ($\eta = \tilde{y}/L$). The $\bar{x} = 91$ position was chosen mainly because it was the farthest downstream station practical to probe in the wind tunnel. Earlier work done with the same wake showed that a semblance of dynamic and thermal wake equilibration had been achieved by $\bar{x} \simeq 60$ as evidenced by the fact that the fluctuations attained predicted 'far wake' levels (see Demetriades 1968*b*) and that the measured velocity and temperature 'defects' reached similarity behaviour (see table 1). It is also noted in table 1 that the flow is always supersonic relative to the probe, and that it has returned to nearly free-stream levels (i.e. the velocity 'defect' $w \equiv (U_\infty - U(0))/U_\infty$, and temperature defect $\theta \equiv (T(0) - T_\infty)/T_\infty$, are small compared with unity). The quantity $\tilde{y}$ is the Howarth–Dorodnitzyn distance, while L is the 'traverse scale' equivalent to Townsend's l_0 (Townsend 1956). In table 2 we furthermore mark the non-dimensional velocity $\tilde{U} \equiv (U_\infty - U)/(U_\infty - U(0))$, to indicate how close the points A, B, etc., lay to the wake axis ($\tilde{U} = 1$) or the free stream ($\tilde{U} = 0$), and the r.m.s. wideband fluctuation magnitudes u' and T', to show the extent of the turbulence spread.

3. Experimental technique

As alluded to in § 1, the correlation of the signals from two hot wires located at separate points in compressible turbulence is a mixture of the correlations of velocity and temperature and their cross-correlation at the two points. The extraction of the velocity and temperature correlations from the signals followed the formal procedure first set forth by Demetriades (1973). Briefly, this procedure, called the 'correlation-mode' technique, requires that the correlation of the two hot-wire signals is recorded for a minimum of four heating-current combinations of the two wires. The technique is of course related to, and actually is a generalization of, Kovasznay's modal analysis (Kovasznay 1950) for a single hot wire, which requires a minimum of three heating-current changes to give the desired variables at a point. For each current change, the variable in a second-degree polynomial is known, so that the three unknown coefficients in the polynomial (the local velocity and temperature fluctuations and their cross-correlation) can be found from the three-equation system. As in Kovasznay's method, the correlation-mode technique requires that the pressure fluctuations are zero if velocity and temperature fluctuations are to be obtained; for a $M_\infty = 3$ wake

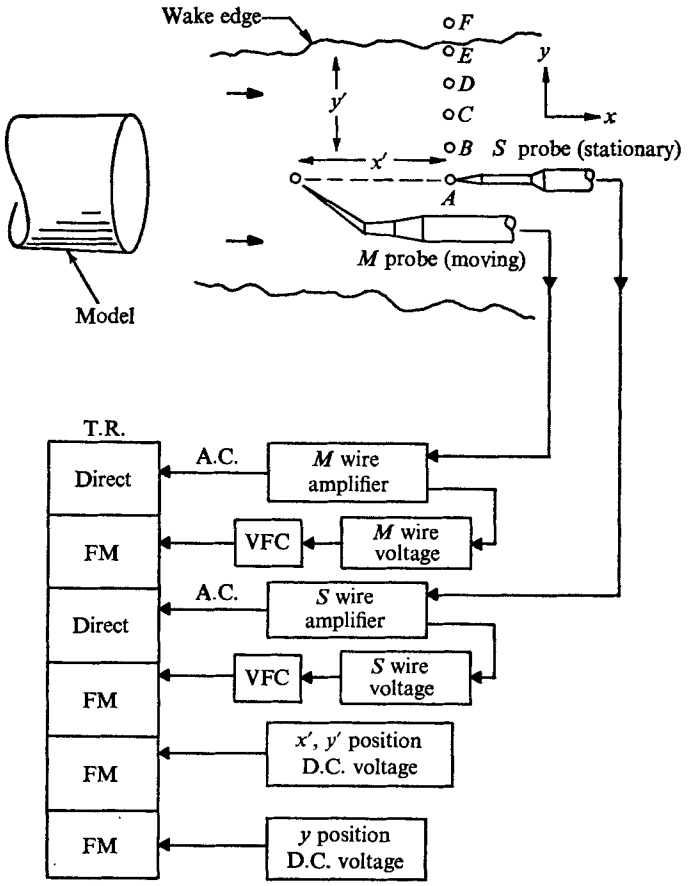

FIGURE 1. Schematic of experiment, showing points of measurement $A, B, \ldots, F$, co-ordinate system and electronic block diagram indicating inputs into 'direct' or 'FM' channels of the tape recorder (T.R.).

this is a fair assumption. As in Kovasznay's method, too, accuracy increases as the number of heating currents increases. Fifteen such combinations were chosen in the present work.

The data were collected by stationing a hot wire S at a point (x, y) in the wake and traversing a second wire M at constant speed away from S along x (the direction of the mean flow) or y (the radial direction), as indicated in figure 1. For the longitudinal correlations x' denotes the instantaneous separation between S and M in the x direction, and for the radial correlations y' denotes their separation along y. Platinum–rhodium wires of diameter 0·00002 in. (20 microinch) and aspect ratio from 150 to 200 were employed. The hot wires were connected to separate, but identical, constant-current compensated amplifiers, set to provide flat response to 2 MHz at a gain ranging to 500.

The two wires were mounted on a probe mechanism immersed in the flow and controlled from the outside of the tunnel. Actuation was provided by a five-degree-of-freedom device, allowing motion of the two-wire pair along x, y or z, and of the M wire along x' and y' in addition. For each correlation, the motion of

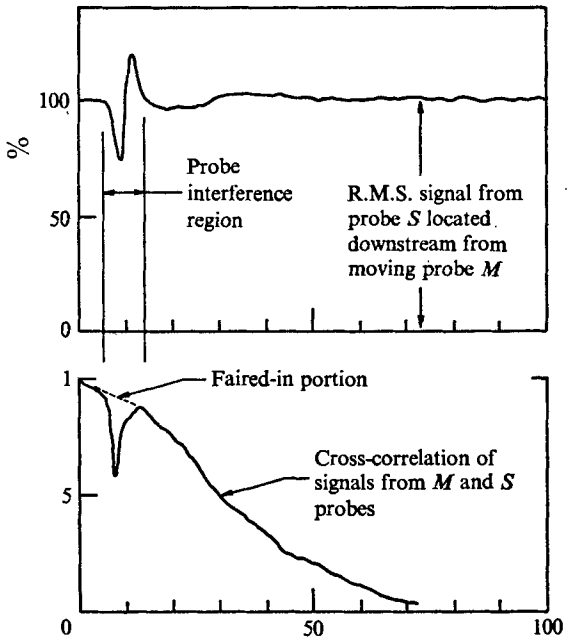

FIGURE 2. Mutual aerodynamic interference of probes.

M away from S was repeated a total of 15 times for 15 different combinations of currents passing through wires M and S. The currents were chosen according to the criteria established by Demetriades (1973). Prior to use, both hot wires were subjected to calibrations in a controlled oven, and their heat-transfer characteristics were measured by calibration in the free-stream Mach 3 flow.

As expected, aerodynamic interference caused distortion of the S probe signal when the M probe found itself upstream of S in a situation depicted in figure 2. This effect was due almost solely to the weak shock waves shed by the upstream probe, rather than to its wake. This interference consisted of a 10–20 % 'ripple' of the S signal whenever that probe found itself lying on the Mach cone of M. The disturbance decreased but was not eliminated by rebuilding the probes to the most slender shape possible. After prolonged tests, it became clear that the disturbance was localized, and so repeatable and recognizable that it could be tolerated. Originally, the wires were separated vertically by a distance of about 0·012 cm; the disturbance occurred in $0{\cdot}03 < x' < 0{\cdot}06$ cm, and was subdued thereafter. During data reduction the disturbance region was left blank, the computer bridging this gap with a straight-line segment.

Earlier spectral data from a similar experiment showed that the wake spectral activity did not extend much beyond 600–700 kHz. This is well within the range of the electronics used, whose high cut-off was the 1·5 MHz limit of the tape recorder. The compensation network of each amplifier was also adequate, since with the floor-to-ceiling ratio of 500 the compensated response of the wires (at wire time constants t_w of 20–50 μs) was in the MHz range also. The problem in

Source	T'	u'	$\overline{uT}/u'T'$
S probe	0·084	0·021	−1
M probe	0·039	0·017	−0·82
Correlation mode	0·046	0·016	−0·83
Earlier data	0·059	0·019	−0·82

TABLE 3. Comparison of fluctuation magnitudes at $y = 0$ computed by various means. Earlier data from Demetriades (1968*b*).

these cases arises from the mismatching of the wire with the compensator, which is unavoidable, as the former traverses regions where its t_w varies. The 'response-restoration' technique (Demetriades 1968*b*) employs a computer program which uses the mean wire voltage to compute the instantaneous departure of t_w from t_c, the set time-constant of the compensator; t_c was initially set equal to t_w as measured just at the outside of the wake. Once t_w and t_c were known, the frequency response of the system wire-compensator was known, and an inverse correction was made by the computer to the turbulent signal.

The correlation-mode and its parent technique, Kovasznay's mode diagram, were used to split the data into velocity and temperature fluctuations. The formulae for the sensitivity coefficients were identical with those of Morkovin (1956). The ingredients for these were computed using the Nusselt–Reynolds number (Nu–Re) calibration in the free stream, done for each individual wire prior to insertion into the wake, coupled with the local Nusselt number Nu measured from the mean-flow data at each point. The resistivity characteristics were computed from the calibration of each wire in a controlled oven, and the local Mach number was taken from the measurement of Demetriades (1968*a*). The assumption was made throughout that the sound intensity is nil. Table 3 shows velocity and temperature fluctuation magnitudes, their cross-correlation as computed by three different methods in the present experiment (two of these are independent), and the corresponding quantities found in 1968. The agreement is judged good, considering that completely different hot wires (0·00002 in. dia. against 0·00005) and electronics were used in the two cases.

It must be understood that the correlation-mode technique does nothing to shorten the labour of resolving the three-dimensional space–time correlation tensor into velocity and temperature contributions. Thus, only a small portion of the correlation features have been so resolved, and this portion will be discussed immediately below. Some further data will also be discussed in their unresolved form.

4. Measurement of auto-correlations

The measurement of auto-correlation, important for testing Taylor's hypothesis by comparison with space correlations, was done in a number of different ways: (i) direct measurement of auto-correlations for wires M and S separately; (ii) by Fourier transformation of spectra measured separately with each wire; and (iii) by cross-correlating the M and S wire signals while the two

sensors were held at the same point. In the first method, a correlation of the type $\overline{ee(\tau)}$ was obtained, where e is the voltage signal and τ the time delay. To restore the frequency response, this correlation was first transformed to

$$R(\tau) \equiv 2\int_{F=0}^{F_{\max}} \left(\frac{\cos 2\pi F\tau}{\mathrm{OTF}} \int_{\tau=0}^{\tau_{\max}} \overline{ee(\tau)} \cos 2\pi F\tau \, d\tau \right) dF \tag{1}$$

by integrating over frequency F. The 'overall transfer function' OTF (Demetriades 1968*b*) operates on the spectrum, which is the Fourier transform of $\overline{ee(\tau)}$. This double transformation (1) is needed basically to account for instrumentation inadequacies, but it also yields the benefit of a smoother correlation curve $R(\tau)$, since integration is equivalent to filtering. Operation (1) was repeated for each of 100 values of the time delay τ of each current for each wire at each point y in the wake. The modes were next separated by curve-fitting, at each τ, a second-degree polynomial to the points (X, Y) in the Kovasznay diagram. Y is now

$$Y^2 \equiv R(\tau)/(e_\sigma^2 V^2), \tag{2}$$

e_σ being the sensitivity to temperature fluctuations, and V the mean voltage across the wire. This curve-fitting, too, was done at each τ for each wire at each point in the wake.

In the second method, the spectra from each probe were Fourier transformed into auto-correlations. The mode-resolution technique was applied 65 times at each of an equal number of frequencies F ranging to approximately 0·7 MHz. For the third method, the delayed signal $e_S(\tau)$ of the S probe was correlated with the undelayed signal from the M probe, to obtain $\overline{e_S(\tau)\, e_M}$ as a function of τ. Response restoration was carried out by first transforming $\overline{e_S(\tau)\, e_M}$ into its cross-spectrum, then replacing OTF (of (1)) by $(\mathrm{OTF})_M^{\frac{1}{2}}(\mathrm{OTF})_S^{\frac{1}{2}}$ before transforming back into correlation space, as

$$R(\tau) = 2\int_{F=0}^{F_{\max}} \left(\frac{\cos 2\pi F\tau}{(\mathrm{OTF})_M^{\frac{1}{2}}(\mathrm{OTF})_S^{\frac{1}{2}}} \int_{\tau=0}^{\tau_{\max}} \overline{e_M e_S(\tau)} \cos 2\pi F\tau \, d\tau \right) dF. \tag{3}$$

The mode-correlation technique was then applied to the correlations $R(\tau)$ by first forming

$$Z \equiv \frac{R(\tau)}{e_{\sigma S} e_{\sigma M} V_S V_M}. \tag{4}$$

V_S and V_M were the mean voltages of S and M, and $e_{\sigma S}$, $e_{\sigma M}$ their temperature sensitivities. The quantity Z is analogous to Y of (2), and was used in the correlation-mode method explained by Demetriades (1973).

5. Longitudinal space correlations

The longitudinal space correlations were resolved for each of the six positions listed in table 2. The technique, analogous to the third method just mentioned for the auto-correlations, consisted of digitizing the quantity $\overline{e_S e_M(x')}$ at 110 points along the full stroke of the M probe ($0 < x' < 0{\cdot}721$ cm). A 'Hanning'

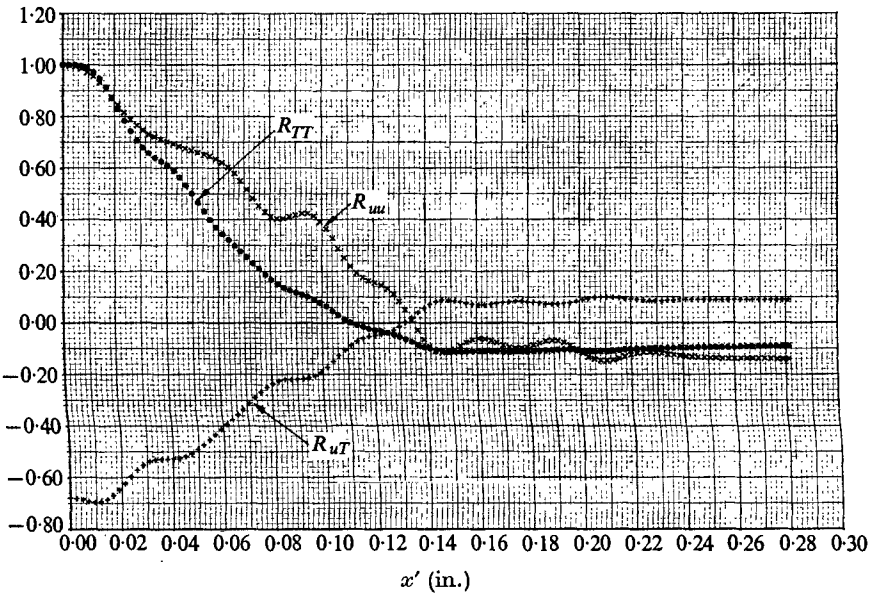

FIGURE 3. Modally resolved, wideband longitudinal space correlation functions.

function (Blackman & Tuckey 1958)

$$H(x') = \tfrac{1}{2}\left(1 + \cos\frac{x'}{0{\cdot}721\pi}\right)$$

was used to weight the measured correlation, so that the final product analogous to (3) was

$$R(x') = 2\int_{F=0}^{F_{\max}} \frac{\cos 2\pi F k x'}{(\mathrm{OTF})_M^{\frac{1}{2}}(\mathrm{OTF})_S^{\frac{1}{2}}}\left(k\int_{x'=0}^{kx'_{\max}} \overline{e_S e_M(x')}\cos(2\pi k F x')\,H(x')\,dx'\right)dF. \tag{5}$$

k is the inverse of a characteristic velocity and

$$Z \equiv \frac{R(x')}{\overline{V_S V_M e_{\sigma S} e_{\sigma M}}}.$$

The modal analysis then gives the dimensional correlations $\overline{u_S u_M(x')}$ and $\overline{T_S T_M(x')}$, and also $\overline{u_S T_M(x')}$ and $\overline{u_M(x') T_S}$, from which, of course, one obtains only the numerators of the desired longitudinal velocity and temperature space correlations:

$$R_{uu}(x', 0, 0; 0) \equiv \frac{\overline{u_S u_M(x')}}{u'_S u'_M(x')}, \quad R_{TT}(x', 0, 0; 0) \equiv \frac{\overline{T_S T_M(x')}}{T'_S T'_M(x')}. \tag{6), (7}$$

The denominators are obtained separately from the r.m.s. voltage signals of the hot wires. Figure 3 shows the sort of longitudinal space correlations (6) and (7) obtained at $y = 0$. The velocity correlation R_{uu} crosses the axis at $x' = 0{\cdot}343$ cm, while the temperature does so a little earlier ($x' = 0{\cdot}279$ cm).

As mentioned by Corrsin (1949), the physical significance of the 'cross-

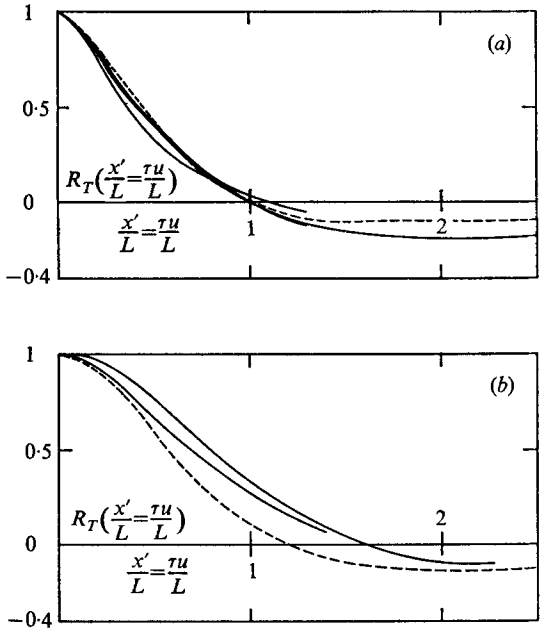

FIGURE 4. Comparison of space (------) and auto-correlations (——) of the temperature fluctuations. (*a*) $y'/L = \eta = 0$ (wake axis). (*b*) $y' = 0{\cdot}61$ cm, $\eta = 3{\cdot}1$ (wake edge).

correlation space correlation' $\overline{u_S T_M(x')}$, as opposed to $\overline{T_S u_M(x')}$, is not always clear. In this paper, we define a 'compound cross-correlation coefficient'

$$R_{uT}(x'\,0,0;0) \equiv \frac{1}{2}\frac{\overline{u_S T_M(x')} + \overline{u_M(x') T_S}}{[\overline{u_S' u_M'(x')}\,\overline{T_S' T_M'(x')}]^{\frac{1}{2}}}.$$

For the longitudinal correlations this becomes

$$R_{uT} = \frac{1}{2}\frac{\overline{u_S T_M(x')} + \overline{u_M(x') T_S}}{\overline{u'T'}}.$$

The intention behind the definition is to recover the usual cross-correlation $\overline{uT}$ at $x' = 0$. Thus, R_{uT} is not by definition unity at $x' = 0$. Figure 3 shows that R_{uT} crosses the axis at a point slightly different from the crossing points of R_{uu} and R_{TT}.

6. Longitudinal correlations and Taylor's hypothesis

Figure 4 summarizes the results for the auto-correlations and the longitudinal space correlations. Because of less scatter only temperature data are shown (i.e. the correlations $R_{TT}(0,0,0;\tau)$ and $R_{TT}(x',0,0;0)$). The abscissa of the former has been converted into a length by setting $x' = \tau U$, where U is the local mean velocity, and all lengths have been in turn normalized by the wake 'transverse scale',

$$L \equiv 0{\cdot}267(C_D A_w)^{\frac{1}{2}} \bar{x}^{\frac{1}{2}}.$$

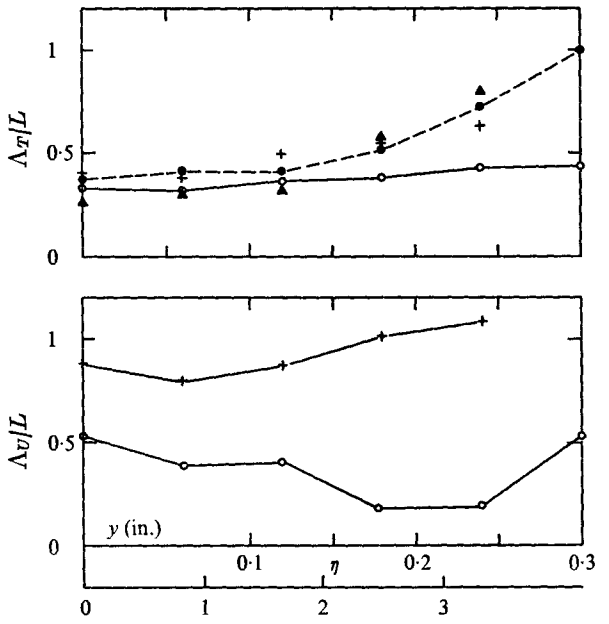

FIGURE 5. Radial variation of velocity and temperature space scales. η, non-dimensional radius. Present data: ○, from space correlation; ●, from auto-correlation (average of all methods); ▲, from auto-correlation (best method). Earlier data: +, from auto-correlation.

Use of this scale is preferred, because it includes implicitly the wake 'drag diameter' $(C_D A)_w^{\frac{1}{2}}$, and because it grows as $\bar{x}^{\frac{1}{3}}$ along the wake. (Another reasonable normalizing length is the r.m.s. wake radius $\bar{y}$, which for this wake was found to be $2{\cdot}1L$.) It is seen that the curves cross the axis in the region $1 < x'/L < 2$. The shape of the correlations does not vary much, and the experimental scatter as represented by multiple solid lines (to account for the different methods of finding $R_{TT}(0, 0, 0; \tau)$, mentioned earlier) is rather small. However, there are differences between auto- and space correlations on the wake edge which do not seem to exist near the axis.

Integral scale lengths computed from these curves are shown in figure 5. The temperature auto-correlations are independent of the method of extracting them from the data; there is also reasonable agreement between the earlier (crosses) and the present data (black points). There are clear differences between auto-correlation and space-correlation scales near the wake edge; this is attributable to the failure of Taylor's hypothesis there. Finally, there is substantial disagreement between the velocity integral scales computed from the auto-correlations and those found from the space correlations. The differences between velocity and temperature integral scales thus appear to be greater if one depends only on spectrum measurements. The space-correlation technique shows the two scales to be about equal and nearly constant at about $0{\cdot}45L$ (nearly $\frac{1}{9}$ the r.m.s. wake diameter) over most of the wake.

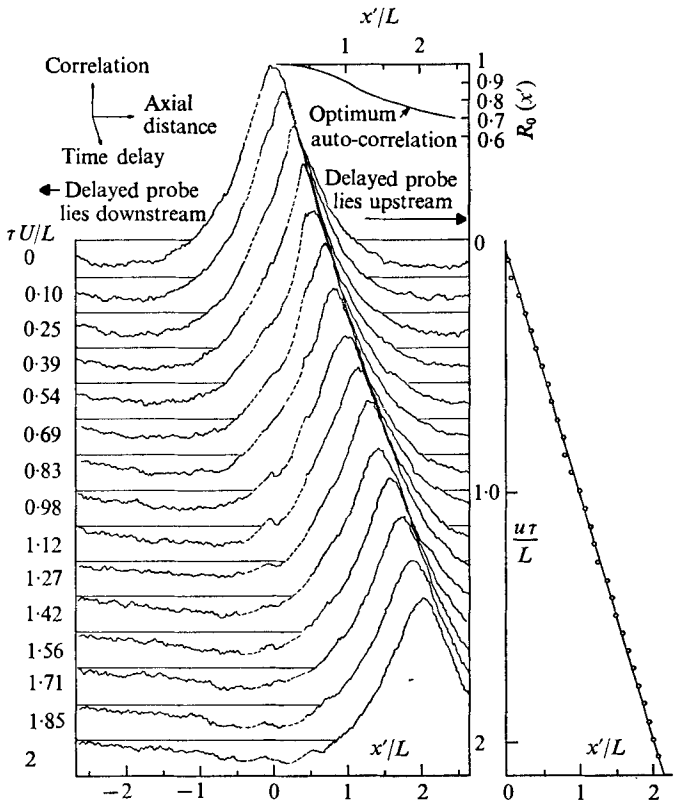

FIGURE 6. Wideband space–time correlations, optimum auto-correlation and eddy convection velocity on the wake axis. $u = dx'/d\tau = 63\,400$ cm s^{-1}.

7. Unresolved correlations

The obvious complexity of the mode-correlation resolution, and of response restoration, motivated a search for features of the correlation structure that could be found without using these techniques. Comparisons were made between restored and unrestored, and resolved and unresolved, correlations. These showed that the differences were rather minor, so that in the present case an approximate notion of some of the more complex features of the wake turbulence can be obtained by looking at the 'raw' signals. The remainder of this paper will present such information.

Figures 6 and 7 show the unresolved, unrestored longitudinal space–time correlations of the hot-wire signal, roughly equivalent to $R_{uu}(x', 0, 0; \tau)$ or $R_{TT}(x' 0, 0; \tau)$, at two positions: $y = 0$ ($\eta = 0$) and $y = 0{\cdot}18$ in. ($\eta = 2{\cdot}32$). Each curve is marked by its non-dimensional time delay $\tau U/L$, and referred to a zero level shown by a straight solid line. The maximum x' range was effectively doubled by alternating the time delay from one wire to another. Two other pieces of information are supplied in each figure: the optimum ('moving-frame') correlation, and the convection velocity of the pattern, found from the slope of the curves on the right. The main item of note in these figures is the upstream–

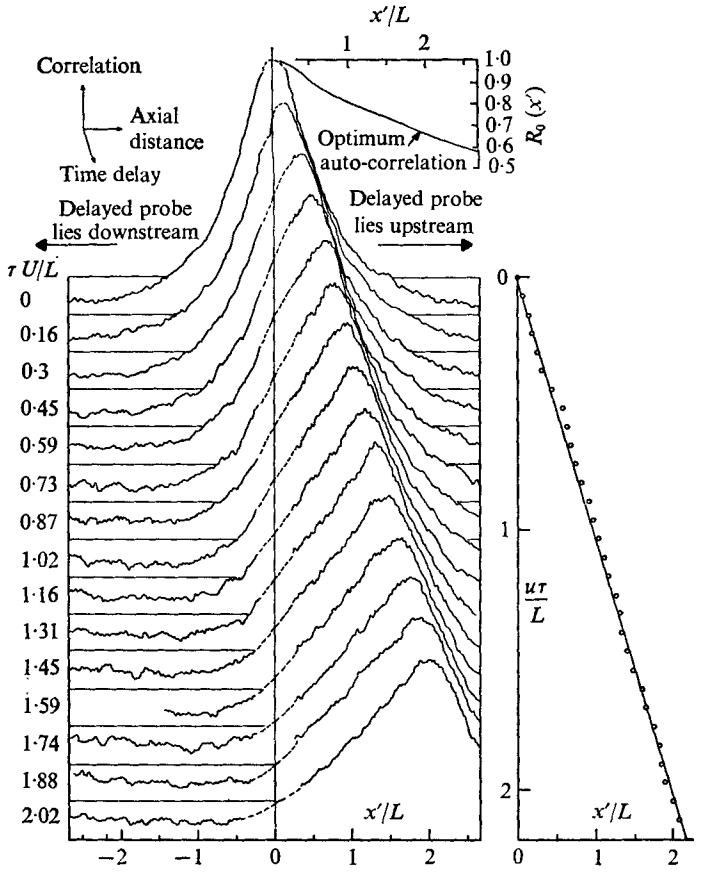

FIGURE 7. Wideband space–time correlations, optimum auto-correlation and eddy convection velocity at the wake edge. $u = dx'/d\tau = 62\,350$ cm s^{-1}.

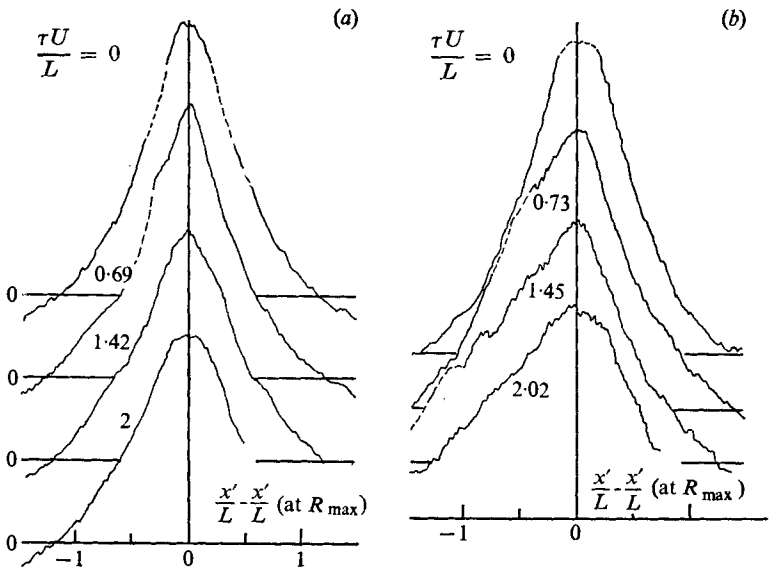

FIGURE 8. Effect of time delay on longitudinal correlation symmetry on the wake axis (left) and at the wake edge (right). (*a*) $\eta = 0$, (*b*) $\eta = 2{\cdot}32$.

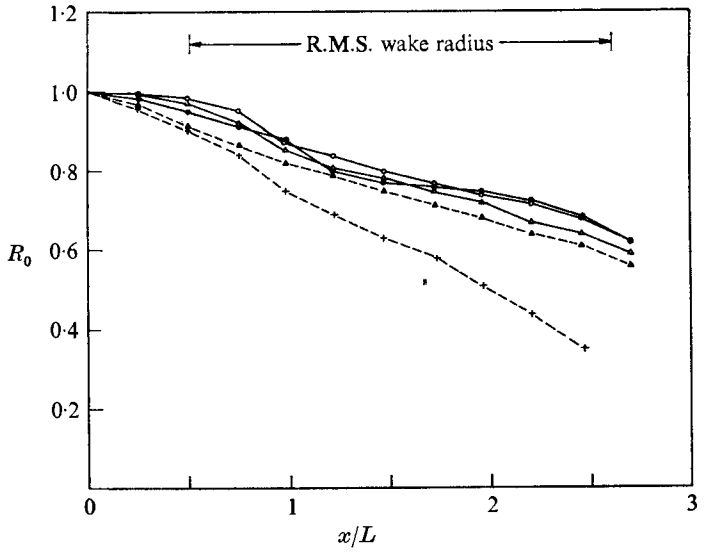

FIGURE 9. Optimum wideband auto-correlation functions at various radial positions.

Radial position	0	0·82	1·56	2·32	3·09
	○	△	●	▲	+

downstream asymmetry evident for the $\eta = 2{\cdot}32$ data. This effect is elaborated upon in figure 8, which plots the correlations at five of the six radial stations studied for a fixed time delay. The asymmetry is obvious beyond $\eta = 1{\cdot}56$.

The space–time co-ordinates of the apex of the correlograms were plotted in an effort to find the convection velocity of the unprocessed correlation pattern, in the manner already illustrated in figures 6 and 7. The velocities so deduced were compared with mean velocities computed earlier from Pitot and static measurements (Demetriades 1968*a*). A difference of 2–3 % between the two sets of data was found. The scatter of the current data and the possibility of changes in the wake flow in the 5-year interim between new and old data, do not allow us yet to ascribe this to differences between flow mean and turbulence convection velocities. However, the accuracy of the measurements was such that the error is not estimated to much exceed this 2–3% difference. The turbulence convection velocity, therefore, is at best nearly equal to the mean flow speed deduced from time-averaged instrumentation.

8. Phenomena in the moving frame

Figure 9 shows the moving-frame (optimum) auto-correlation $R_0(x')$ for five radial positions. We see that the decay process is quite uniform inside the wake, up to about $\eta = 2{\cdot}3$. The $\eta = 3{\cdot}09$ datum indicates a much faster decay process near the wake edge. Since a fast-decreasing $R_0(x')$ implies an unfrozen turbulence pattern, this datum states that Taylor's hypothesis is worst near the wake edge, a conclusion independently expressed earlier from the study of auto-correlations, space correlations and their various scales. Unfortunately, the probe stroke (i.e. the maximum x') was insufficient to reach distances where $R_0(x')$ is near zero, so

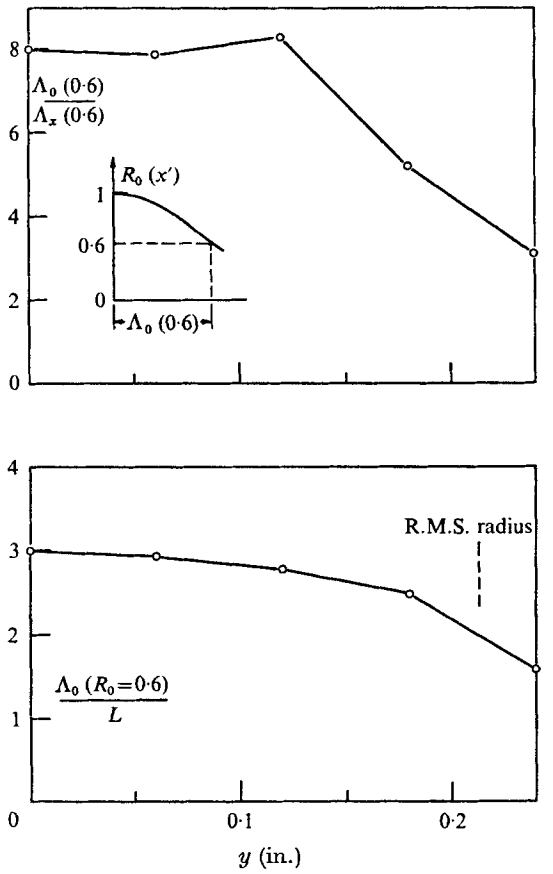

FIGURE 10. Optimum correlation scale as compared with the space scale (top) and the wake transverse scale (bottom).

that the final decay stages remain unknown. To put the decay process in quantitative terms, we have thus resorted to plotting the value of x' at which R_0 has decreased to 0·6. This x' value is called the 'auto-correlation length scale' Λ_0; it is plotted in figure 10. To enhance the meaning of this scale, we should actually compare it with a corresponding space scale such as Λ_U or Λ_T. This has also been done in figure 10, with the added expedient of discarding Λ_U and Λ_T in favour of Λ_x ($x' = 0{\cdot}6$), a representative integral scale length at which longitudinal space correlation functions are down to 0·6. The ratio $\Lambda_0(0{\cdot}6)/\Lambda(0{\cdot}6)$, indicating the number of their own 'lengths' eddies travel before they decay, is about 8 inside the wake, but decreases to about 3 at its edge. We note the interesting fact, emerging from figures 4, 5 and 9 and 10, that, for scale ratios Λ_0/Λ_x of order 8, the use of Taylor's hypothesis is apparently legitimate, even though the optimum auto-correlations by themselves indicate a decaying turbulence process.

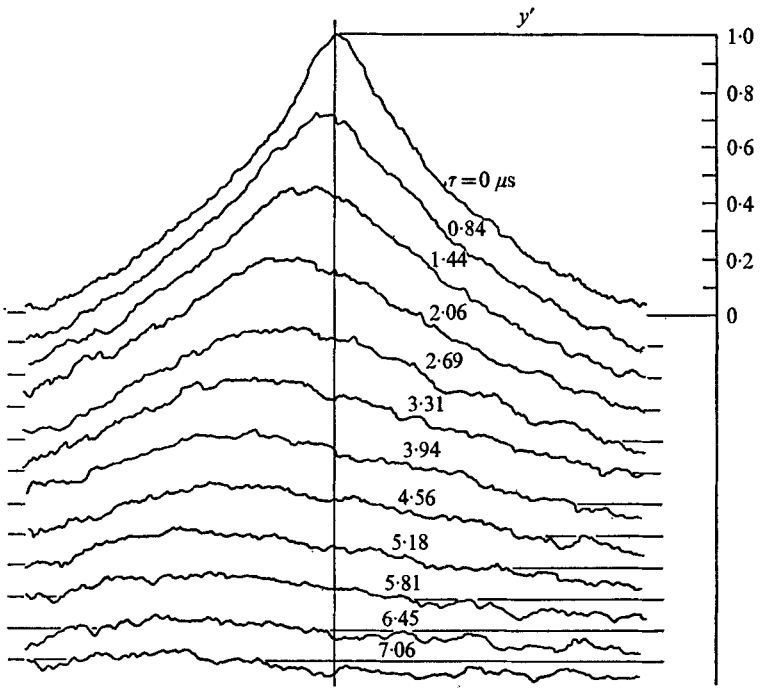

FIGURE 11. Radial wideband space correlations near the maximum shear region. $y = 0{\cdot}305$ cm, $\eta = 1{\cdot}56$. y' in arbitrary units.

9. Radial space–time correlations

Unresolved, unrestored radial space–time correlations $R(0, y', 0; \tau)$ were measured at five of the six radial positions. Figure 11 shows such typical correlograms for twelve values of the time delay at $y = 0{\cdot}305$ cm ($\eta = 1{\cdot}56$), which lies close to the maximum-shear zone. Zero levels are again shown by straight lines for each value of τ. The effective stroke of the moving probe M is again doubled by switching the time-delay circuit from one probe to another.

The zero-delay ($\tau = 0$) curve in figure 11 is the unresolved radial counterpart of the space correlations discussed earlier, for the radial position $\eta = 1{\cdot}56$. Although this curve does not seem to become negative within the bounds of the probe stroke, it should be noted that the latter is shorter than the longitudinal stroke. Comparison of the positive portion of both radial and longitudinal correlations plotted against physical distance showed them to coincide approximately. This is rather surprising since the radial velocity correlations are usually quite contracted relative to the longitudinal velocity correlations in incompressible isotropic flows. However, the correlations discussed here were not resolved modally, and the conclusion of anisotropy, however likely, cannot be definitely made.

For $\tau > 0$ the correlations show a maximum on the left of $y' = 0$, in the region where the time delay is switched to the M probe. In this example, as the S probe is fixed at $y = 0{\cdot}305$ cm and the delayed M probe is moved from the wake centre

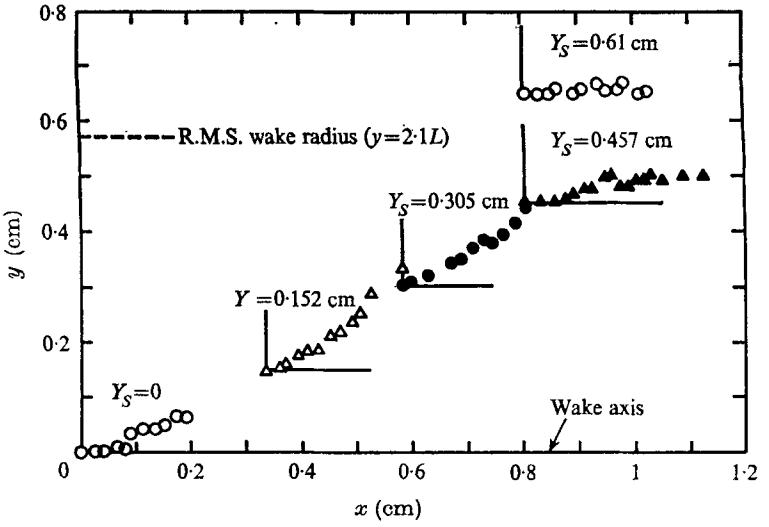

FIGURE 12. Mapping of the 'outline of an eddy' using the radial space–time correlation maxima, represented by points.

towards the wake edge, the correlation has a maximum at some distance $y > 0{\cdot}305$ cm. The maximum moves systematically outwards to greater y as the time delay is increased. Now the turbulence convection velocity is already known to be quite uniform across the wake; with this velocity in mind, the time delays τ, labelling each curve of figure 11, can be replaced by equivalent longitudinal distances x'. The locus of the maxima in this figure is then a line in the x', y' (or x, y) plane. The explanation attached to this line is that it represents, roughly, the 'centre-line' of a large eddy, and that this eddy is therefore inclined relative to the wake axis. The inclination is here pictured in the wrong quadrant; the eddies actually are 'pointing' downstream.

By piecing together the local eddy inclination at various distances from the wake axis, a composite picture of the axis of such an eddy was put together, as shown on figure 12. The axis is inclined to the wake axis at some angle of order 25°; thereafter, the inclination angle increases slightly, but it decreases to zero at the wake edge, where the tops of the eddies appear finally parallel to the flow axis.

10. Conclusions

A number of important lessons regarding experimental technique were learned in this experiment. The correlation-mode technique of hot-wire anemometry was applied successfully in a compressible flow. Aerodynamic interference by the upstream probe in a two-probe system was found to be significant, but its clarity and repeatability made it easy to recognize and correct for. Even so, a rigorous hot-wire anemometer correlation measurement in compressible flows is a difficult and time-consuming task. However, some geometrical features of this particular flow were discernible without full recourse to every facet of the technique.

The following was learnt about the correlation structure of the wake:

(i) Taylor's hypothesis is weakest near the wake edge. (ii) Whereas single-point (Eulerian spectrum or auto-correlation) measurements had earlier given differences between velocity and temperature scales, the space correlations showed these two scales about equal, at about $0{\cdot}45L$. (iii) The space correlation functions show an upstream–downstream asymmetry. (iv) At any point in the wake, the unfiltered eddy convection velocity equals the mean flow velocity within the accuracy of the measurement. (v) On the wake axis, the eddies move a distance almost an order of magnitude greater than their own size before they decay appreciably. (vi) There are provisional indications that the radial and longitudinal space correlation functions are nearly equal. (vii) The characteristic eddy structures appear as elongated forms, inclined at an angle of about 25° to the flow vector on the axis, but bending parallel to the axis at the wake edge.

This work was supported jointly by the Advanced Research Projects Agency and the U.S. Air Force under contract F04701-71-C-0035. The author is indebted to Mr Lee Von Seggern for his assistance with the electronic instrumentation and design of the electromechanical actuator mounting the hot-wire probes.

REFERENCES

Blackman, R. B. & Tuckey, J. W. 1958 *Measurement of Power Spectra.* Dover.
Corrsin, S. 1949 *N.A.C.A. Tech. Note*, no. 1864.
Demetriades, A. 1968*a* *A.I.A.A. J.* **6**, 432.
Demetriades, A. 1968*b* *Phys. Fluids*, **11**, 1841.
Demetriades, A. 1968*c* *J. Fluid Mech.* **34**, 465.
Demetriades, A. 1973 *J. Appl. Mech.* **40**, 822.
Fox, J. 1968 *A.I.A.A. J.* **6**, 233.
Kovasznay, L. S. G. 1950 *J. Aero. Sci.* **17**, 565.
Lane, F. 1967 *A.I.A.A. J.* **5**, 2193.
Morkovin, M. V. 1956 *Agardograph*, no. 24.
Townsend, A. 1956 *The Structure of Turbulent Shear Flow.* Cambridge University Press